

ARTICLE

Analysis of Heat Transfer Phenomena inside Concrete Hollow Blocks

Joelle Al Fakhoury^{1,2} Emilio Sassine^{1*} Yassine Cherif² Joseph Dgheim¹ Emmanuel Antczak² Thierry Chartier²

1. Lebanese University, Habitat and Energy Unit, Group of Mechanical, Thermal and Renewable Energies - Laboratory of Applied Physics (LPA-GMTER), Faculty of Sciences, Fanar Campus, Lebanon

2. University Artois, IMT Lille Douai, Junia, University Lille, ULR 4515, Laboratoire de Génie Civil et géo-Environnement (LGCgE), F-62400, Béthune, France

ARTICLE INFO

Article history

Received: 9 March 2022

Revised: 28 March 2022

Accepted: 20 April 2022

Published Online: 10 May 2022

Keywords:

Hollow block

Cavities

Thermophysical properties

Dynamic boundary conditions

3D modelling

ABSTRACT

During both hot and cold seasons, masonry walls play an important role in the thermal performance between the interior and the exterior of occupied spaces. It is thus essential to analyze the thermal behavior at the hollow block's level in order to better understand the temperature and heat flux distribution in its structure and potentially limit as much as possible the heat transfer through the block. In this scope, this paper offers an experimental and numerical in-depth analysis of heat transfer phenomena inside a hollow block using a dedicated experimental setup including a well-insulated reference box and several thermocouples and fluxmeters distributed at the boundaries and inside the hollow block. The block was then numerically 3D modelled and simulated using COMSOL Multiphysics under the same conditions, properties, and dimensions as the experimentally tested block. The comparison between the numerical and experimental results provides very satisfactory results with relative difference of less than 4% for the computed thermal resistance.

1. Introduction

Energy consumption in buildings is strongly increasing lately due to population growth, economic development and improved living standards. These different causes put additional pressure on the energy system. This consumption mainly includes space heating and cooling. For

example, the use of heating in Lebanon presents the most interesting share of household energy consumption in Lebanon in 2012, it is approximately almost half of the total energy consumption. And that the equipment rate of air conditioner presents a strong increase from 16% to 55% from 2000 to 2012^[1]. The energy consumption of air conditioning and heating systems depends on several factors,

*Corresponding Author:

Emilio Sassine,

Lebanese University, Habitat and Energy Unit, Group of Mechanical, Thermal and Renewable Energies - Laboratory of Applied Physics (LPA-GMTER), Faculty of Sciences, Fanar Campus, Lebanon;

Email: emilio.sassine@gmail.com

DOI: <https://doi.org/10.30564/jbms.v4i1.4500>

Copyright © 2022 by the author(s). Published by Bilingual Publishing Co. This is an open access article under the Creative Commons Attribution-NonCommercial 4.0 International (CC BY-NC 4.0) License. (<https://creativecommons.org/licenses/by-nc/4.0/>).

one of the most important factors is the heat transfer through the building envelope. In this context, the thermal performance in masonry walls is taken into account in this study, especially since the energy efficiency of buildings is an area that has become very important in the context of energy conservation.

Nowadays, hollow blocks are one of the most used materials in building envelopes for what the advantages they offer in terms of cost, ease of implementation, weight, fire resistance, thermal and sound insulation, and acoustic insulation. For example JJ del Coz Díaz et al. [2] presented a comparative nonlinear thermal analysis for a total of eighteen different in situ cast floors by varying both the constituent materials and the shape of the hollow blocks using the finite element method (FEM). They concluded that the overall heat transfer coefficient increases with increasing material conductivity. In addition, there is a growing interest in using materials with good physical properties for energy conservation. Ribeiro et al. [3] analyzed the sound insulation on a masonry wall built with hollow concrete blocks and construction and demolition waste as aggregates using the reverberant chamber method with the aim of providing sound insulation in indoor environments. They concluded that all types of panels increased the weighted sound reduction index. M. Fringuellino et al. [4] described the characteristics of sound transmission through hollow walls, with the aim of analyzing the sound reduction index on several types of walls with different thicknesses and materials, using the equation based on the familiar formula for the normal incidence transmission of a longitudinal wave at the intersection between different materials. They concluded that the material properties of the complex structure of the block can strongly influence the sound reduction index at the low and high frequency. Yang et al. [5] investigated the sound insulation properties of a concrete hollow brick wall through experimental research and theoretical analysis. They concluded that concrete hollow brick not only has excellent mechanical properties but also excellent sound insulation properties due to its rational hole shape design. Fraile-Garcia et al. [6] studied the acoustic behavior of waste-tire rubber concrete bricks, lattice joists and hollow blocks with different proportions of rubber in the mix using the difference between transmitted and emitted levels method. They proved that highly doped elements are an excellent option for isolating low frequency sounds, while intermediate and standard elements are a more attractive option for blocking medium and high frequency sounds.

Numerical heat transfer modeling is necessary to characterize the thermal parameters of the hollow block. Numerical methods allow to apply the heat transfer equation

in steady state or dynamic conditions. Díaz et al. [7] used the finite element method (FEM) for the design optimization of lightweight hollow blocks with the aim of saving energy. They concluded that by increasing the number of vertical and horizontal intermediate bulkheads and decreasing the conductivity of the material, they obtained the best thermal efficiency. A. Antar et al. [8] studied numerically the heat transfer through a hollow block. They concluded that with increasing the number of cavities the heat loss decreased, while keeping the block width constant. Urban et al. [9] analyzed the thermal performance of masonry wall systems for six different geometries with different densities by utilizing a finite difference computer modeling. They concluded that the use of lightweight concretes in the production of concrete masonry units is therefore one of the most effective ways to improve their thermal performance. M. Mahmoud et al. [10] developed a computational fluid dynamics (CFD) model, to determine the size and distribution of cavities in building blocks, which can reduce the variation of the heat flux through the walls as much as possible and thus to obtain energy savings in air conditioning. The results showed that the variation of the heat flux depends on the size of the cavities and blocks. Heinrich Manz [11] studied the heat transfer by natural convection of air layers in vertical rectangular cavities using a computational fluid dynamics (CFD) code. This study has provided the starting position for future applications of the code to more complex cases of facade elements. Fogiatto et al. [12] studied the thermal transmittance for different cavity configurations of hollow concrete blocks by performing CFD simulations. The results showed that larger cavities provide the higher transmittance values and that the radiation effect can play an important role in the overall heat transfer through blocks. Zhang et al. [13] analyzed the thermal performance of a hollow concrete wall using MATLAB program. The results showed that by reducing the number of cavities in each row, the thermal performance could be improved. S. Al-Tamimi et al. [14,15] used a finite element analysis using ABAQUS software to determine the optimal hole geometry for concrete bricks that would increase the thermal resistance of the wall and thus reduce electrical energy consumption. They concluded that there is an effect of the hole shape on thermal resistance and then an effect on heat flux reduction. Then, they developed a finite element model (FEM) with the aim of determining the optimal geometry of cavities and their arrangement in concrete masonry blocks to reduce the heat flux. They concluded that the simulation results are promising and indicated that the new optimal cavity geometry design was much better than commercially available cavity blocks. J. Xamán et al. [16]

studied the thermal analysis of a hollow block with/without insulation and reflective roofing materials for 24 h in the hottest and coldest days, considering environmental variables of a Mexican city with warm weather using the finite volume method. The results showed the interest of using the combination of an insulating material and a reflective coating on roofs with hot weather. Chihab et al.^[17] numerically investigated the thermal inertia of different roof configurations constructed with traditional concrete blocks used in Morocco with three and six cavities, using the Galerkin finite element method. The results indicated that the combined emissivity and interior heat transfer coefficients have a significant impact on the thermal inertia of the roof. JJ del Coz Díaz et al.^[18] described the development of a new type of hollow concrete masonry block unit to minimize its weight based on topological optimization using the finite element method (FEM). The numerical results gave rise to new solutions in masonry construction through proper block pre-design.

In addition to numerical simulations, many experimental methods have been developed by researchers to estimate thermal performance in building envelopes such as thermal conductivity, thermal resistance, under controlled or real conditions. Among these studies, Hu et al.^[19] constructed 6 groups of hollow brick model blocks with different filling positions and filling rates using a cold and hot test box, with the aim of improving the insulation performance of hollow brick, in the continuous operation of air conditioning in the cold regions of China in winter. They concluded that with the filling of the hollow block with EPS insulating material is better at improving the insulation performance of the hollow brick block. Wu et al.^[20] investigated the mechanical and thermal properties of rectangular hollow blocks using the hot box method. They concluded that the use of this block could not only reduce the energy consumption but also decrease the pressure on the environment.

Finally researchers have studied experimentally and numerically the heat transfer in the building envelope, for example Sassine et al.^[22-24] proposed an experimental and numerical analysis of the thermal performance of Lebanese hollow block concrete. Then, they investigated the effect of adding expanded polystyrene (EPS) beads to the solid mixture of hollow block concrete by numerical and experimental approaches. They concluded from the numerical results is that the three-dimensional (3D) model has visualized the heat flux and temperature distribution in the block as well as the air velocity and convective heat exchange inside the cavities of the block. And from the

experimental results, they showed that the thermal resistance of the block can almost double by adding 18 g of polystyrene beads to the concrete mix.

This paper focuses particularly on the heat transfer phenomena inside hollow blocks by instrumenting an experimental setup and measuring local temperatures and heat fluxes in a 49 cm × 19 cm × 10 cm hollow block having four rectangular cavities under controlled conditions using the thermostatic baths in an experimental heating box setup. In the first part of the paper, the equivalent thermal properties of the hollow block and the concrete mixture are determined, namely the thermal conductivity, the density, and the specific heat. Then, in the second part, the detailed heat transfer is studied both experimentally and numerically through heat flux sensors and temperature sensors placed across the studied sample.

2. Standard Thermal Characterization Setup

2.1 Description of the Experimental Setup

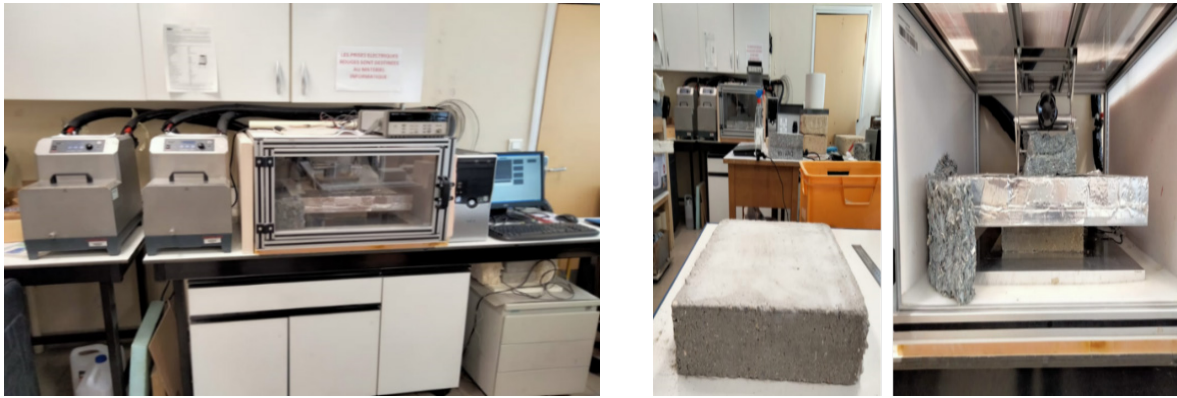
2.1.1 Experimental Setup

A standard experimental setup is used to determine the thermal properties of building materials in the LGCgE laboratory. The samples are placed horizontally between two aluminum plates and the heat transfer through the hollow block is measured using a fluxmeter method in a well-insulated reference box.

The heat exchange plates are connected by two thermostat baths as shown in Figure 1a. Such that one is connected to the upper plate at a temperature of 25 °C and the other is connected to the lower plate at 15 °C. The flux and temperature measurement are performed by two flux meters of 0.15 × 0.15 m² area and two T-type thermocouples, which are placed below and above the sample respectively. The upper plate can be moved vertically with the help of a support that in turn allows keeping this system in place. The thermal properties to be determined are the thermal conductivity (λ) and the specific heat (CP).

The tested samples were wrapped laterally with a recycled wool insulation material as shown in Figure 1b, in order to reduce lateral heat loss and ensure unidirectional heat transfer.

The thermal properties of the hollow block, namely the thermal conductivity (λ) and the specific heat (CP), were determined using the fluxmetric method (NF EN 12664^[21]), in which the sample is placed between two aluminum plates connected to thermostatic baths allowing to impose controlled boundary conditions on the sample. Two fluxmeters and two thermocouples are placed above



(a) (b)
Figure 1. Experimental setup for thermal characterization

and below the block to measure the heat flux and the temperature respectively. The thermocouples and fluxmeters are connected to a data acquisition center allowing to visualize the evolution of the heat flux and temperature on each face of the block.

2.1.2 Tested Specimens

Two specimens were tested using the standard thermal characterization setup: a concrete mixture sample taken from the hollow block, and the hollow block itself.

To thermally characterize the concrete constituting the hollow block, a sample was prepared by cutting three rectangular pieces from the hollow block and gluing them together using a very thin mortar glue as shown in Figure 2a. The parallelepiped obtained sample is 16.5 cm × 7 cm × 6.5 cm; this provides a sample with sufficient thermal resistance for the measurement method.



(b)
Figure 2. Tested samples: concrete solid mixture (a) and hollow block (b)

The studied hollow block has a length of 49 cm, a height of 20 cm and a width of 10 cm and contains 4 cavities in series as shown in Figure 2b.

The main ingredients in the production of normal weight hollow block are: natural aggregates, cement and water. The aggregate mixture is made of 25% of fine gravel aggregates (4 mm–8 mm) and 75% of powdered stone dust (0.5 mm–4 mm). The dosage of the mixture is made such as 1 m³ of aggregates is mixed with 50 kg of Portland cement and 50 L of water to form the solid concrete mixture.

It is a block molded and pressed by a pressing mold in different forms. In our case we considered a block of parallelepiped (24.7 cm × 10 cm × 19cm) and formed by rectangular cavities (Figure 2b).

It is important to highlight that the thermal properties of the hollow block that are determined from experimental measurements are equivalent thermal properties since the



(a)

sample is composed of a concrete matrix and air contained in the cavities of the sample.

2.2 Characterization Method

2.2.1 Determination of the Density

The equivalent densities of the samples were determined by dividing weight of the samples (determined using a digital balance) by its volume (length \times width \times thickness).

2.2.2 Determination of the Thermal Conductivity

The thermal conductivity represents the ability of a material to let heat pass or on the contrary to oppose to it. Because of the difference in temperature on each side of the sample under test, a heat transfer exchange exists. Once the steady state is reached, one can calculate the thermal conductivity (λ) such as $\lambda = \frac{e}{R}$ with e is the thickness of the sample studied in m , R is the thermal resistance in $m^2.K/W$, and λ is the thermal conductivity in $W/m.K$. Then the higher the thermal conductivity, the more heat the material allows to pass and therefore it is less insulating.

The flux and temperature were measured simultaneously on each block face and then the resistance R was calculated using Fourier's law in a unidirectional steady state system, such as;

$$\varphi_1 = \frac{\Delta\theta}{R} \quad (1)$$

$$\varphi_2 = \frac{\Delta\theta}{R} \quad (2)$$

$\Delta\theta$ is the temperature difference.

Once we determine the flux variation, we can calculate its sum $\Sigma\varphi$, and then the thermal resistance R , such that;

$$\Sigma\varphi = \frac{2}{R} \Delta\theta \quad (3)$$

$$\Rightarrow R = \frac{2 \Delta\theta}{\Sigma\varphi} \quad (4)$$

Finally, we can calculate the thermal conductivity, using the following formula;

$$\lambda = \frac{e}{R} \quad (5)$$

The thermal conductivity is determined when the sum of the fluxes stabilizes.

2.2.3 Determination of the Specific Heat

The specific heat C_p is designated by the amount of heat stored in a material, i.e. it is expressed by the heat capacity C . This means that when the heat capacity in-

creases, a large amount of energy can be stored but the temperature becomes less important. Note that for the same sample the value of the specific heat varies with the temperature.

This amount of energy Q can be calculated from an initial state $t_{initial}$ steady state and then changing the temperature set point on one or both sides, so that our system reaches the steady state again, in which the material has returned to its stable state at a final state t_{final} , we can calculate Q ;

$$Q = \int_{t_{initial}}^{t_{final}} \Delta\varphi dt \quad (6)$$

$\Delta\varphi$ expresses the difference in fluxes. dt denotes the time step, in our case we considered $dt = 10 \text{ sec}$. Q is the energy stored in the sample during the transient phase, it is expressed in J .

As well as, the heat capacity (C) is obtained by dividing the amount of energy supplied (Q) by the temperature difference ($\Delta\theta$), such that;

$$C = \frac{Q}{\Delta\theta} \quad (7)$$

C is expressed in (J/K) , $\Delta\theta$ presents the difference between the average temperature in the final state and the average temperature in the initial state, i.e. that;

$$\Delta\theta = \overline{\theta_{final}} - \overline{\theta_{initial}} \quad (8)$$

If the heat capacity increases, this means that a large amount of energy can be stored, relatively low temperature.

Finally, knowing the heat capacity C , the density of the sample ρ and its thickness e , then;

$$C_p = \frac{C}{\rho.S.e} \quad (9)$$

ρ is expressed in kg/m^3 , S is the surface area of the sample in m^2 , e is the thickness of the tested sample in m , C_p is the specific heat capacity expressed in $J/Kg.K$.

Note that the specific heat C_p is different for each material and according to the physical state (solid, liquid and gas).

The specific heat is determined when the difference of the flux is stable.

2.3 Experimental Results

2.3.1 Thermal Properties of the Concrete Mixture

The concrete solid mixture of the block sample has a density of $\rho = 2150 \text{ Kg/m}^3$.

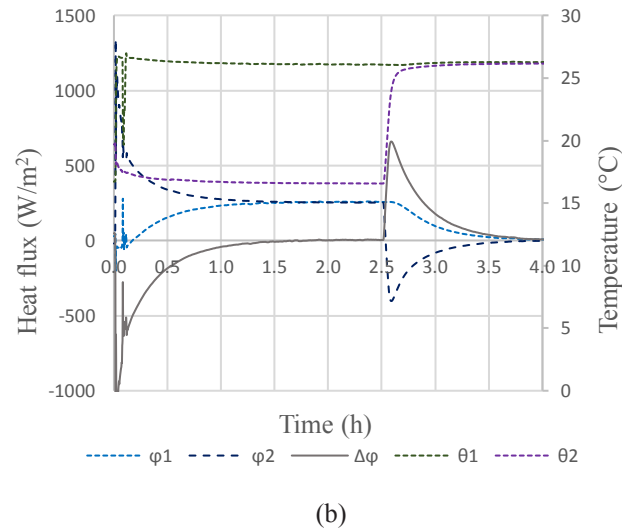
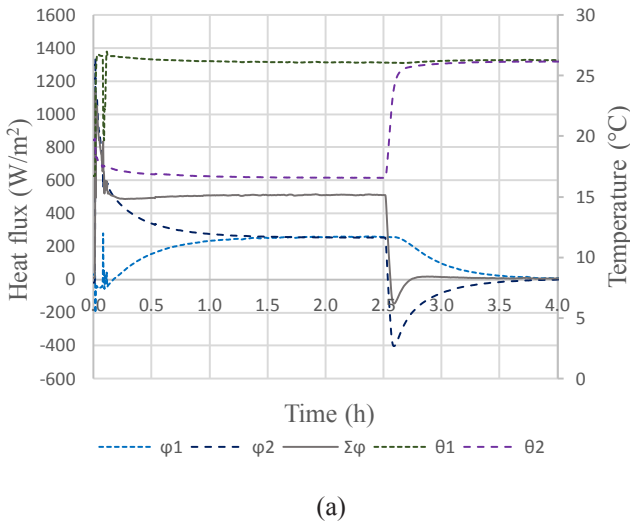


Figure 3. Determination of thermal conductivity (a) and the specific heat (b) of the concrete mixture

At first, a different temperature difference was imposed such that $\theta_1=25\text{ }^\circ\text{C}$ and $\theta_2=15\text{ }^\circ\text{C}$, in order to determine the thermal conductivity of the sample. After 1h30, the steady state is reached and the heat fluxes at the boundaries of the sample ϕ_1 and ϕ_2 are approximately equal to 254 W/m^2 (Figure 3a). After reaching the steady state conditions, the temperature condition θ_2 is increased to $25\text{ }^\circ\text{C}$, in order to determine the specific heat of the sample. The heat fluxes ϕ_1 and ϕ_2 decrease and converge to an approximately zero value (Figure 3b).

By using Equations (4), (5) and (9) the thermal conductivity and the specific heat can be computed: $\lambda = 1.6\text{ W/m.K}$ and $C_p = 1392.82\text{ J/m.K}$.

2.3.2 Equivalent Thermal Properties of the Hollow Block

The density equivalent density of the hollow block is

$$\rho = \frac{m}{V} = \frac{11.3}{0.49 \times 0.19 \times 0.1} = 1213.75\text{ Kg/m}^3.$$

Two tests were performed for the determination of the thermal properties of the hollow block. In the first one (1), the two fluxmeters were placed in the middle of the block on both sides of the block. In the second (2), the fluxmeters are placed on both sides of the cavity as shown in Figure 4.

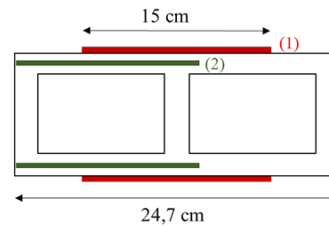


Figure 4. Fluxmeters locations in the two tests

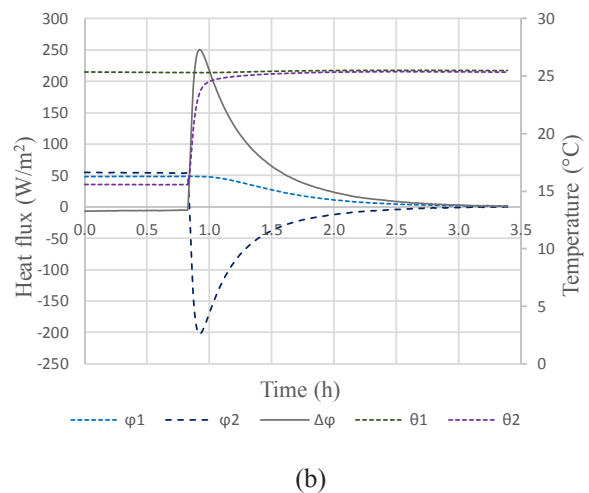
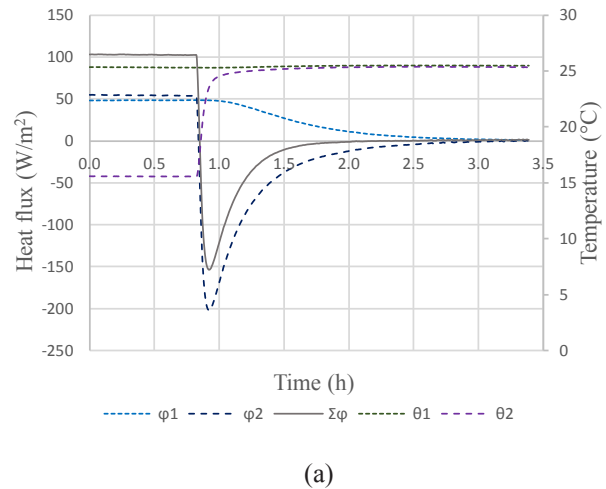


Figure 5. Determination of thermal conductivity (a) and the specific heat (b) of the hollow block in the 1st test

According to Equations (4) and (5) and Figure 6a;

$$R = \frac{2 \Delta \theta}{\Sigma \varphi} = \frac{2 \times 9.77}{104} = 0.188 \text{ m}^2 \cdot \text{K}/\text{W}$$

$$\Rightarrow \lambda = \frac{e}{R} = \frac{0.1}{0.188} = 0.53 \text{ W}/\text{m} \cdot \text{K}$$

From Equation (9) and Figure 6b, $C_p = \frac{c}{\rho \cdot S \cdot e} = \frac{92107.57}{1213.96 \times 1 \times 0.1} = 758.73 \text{ J}/\text{Kg} \cdot \text{K}$.

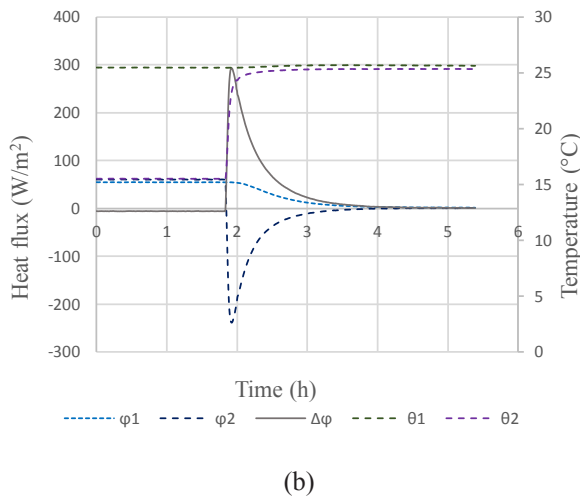
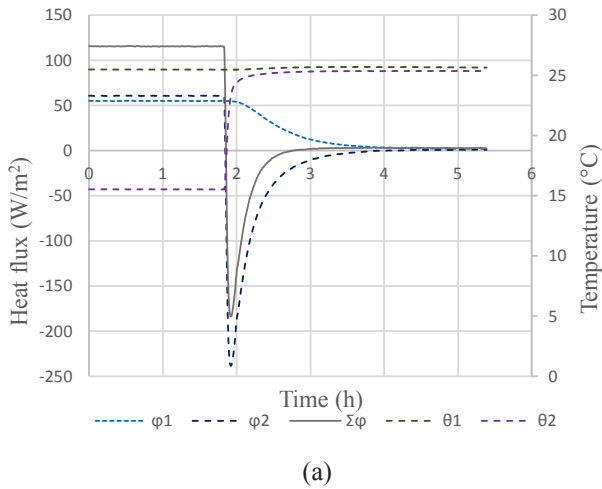


Figure 6. Determination of thermal conductivity (a) and the specific heat (b) of the hollow block in the 2nd test

According to Equations (4) and (5) and Figure 6a, $R = \frac{2 \Delta \theta}{\Sigma \varphi} = \frac{2 \times 9.9}{115} = 0.172 \text{ m}^2 \cdot \text{K}/\text{W} \Rightarrow \lambda = \frac{e}{R} = \frac{0.1}{0.172} = 0.58 \text{ W}/\text{m} \cdot \text{K}$.

According to Equation (9) and Figure 6b $C_p = \frac{c}{\rho \cdot S \cdot e} = \frac{99971.01}{1213.96 \times 1 \times 0.1} = 823.51 \text{ J}/\text{Kg} \cdot \text{K}$

So far, as a first conclusion, the thermal conductivity obtained in test 2 is approximately greater than that in the first one. This can be justified by the fact that in the second test, the fluxmeters were placed on two sides where there are more materials.

Table 1 summarizes all the thermal properties of the

tested samples. The results show that the location of the sensors between tests 1 and 2 has a slight impact on the thermal conductivity (8%) and the specific heat (8%).

Table 1. Thermal properties of the tested materials

Material	ρ (Kg/m ³)	λ (W/m.K)	C_p (J/Kg.K)
Hollow block (configuration 1)	1214	0.53	758.73
Hollow block (configuration 2)	1214	0.58	823.51
Concrete mixture	2150	1.6	1393

3. Detailed Heat Transfer Phenomena in the Hollow Block

3.1 Description of the Experimental Setup

After the determination of the equivalent thermal properties of the block and the solid part of the hollow block, a particular attention was given to the analysis of the heat transfer inside the hollow block. A particular experimental setup was built for this purpose where the block was placed between two flat plates and the assembly was well insulated using polyurethane and wood to ensure a unidirectional transfer in the system (Figure 7).

The temperature in the box varies in a step shape between 10 °C and 50 °C. It is covered by 16 cm of polyurethane insulation and 1.5 cm of wood on the borders of the box.

The block is well insulated to ensure a unidirectional heat transfer created by the difference in temperature between the two edges of the block from the hotter side to the colder side.

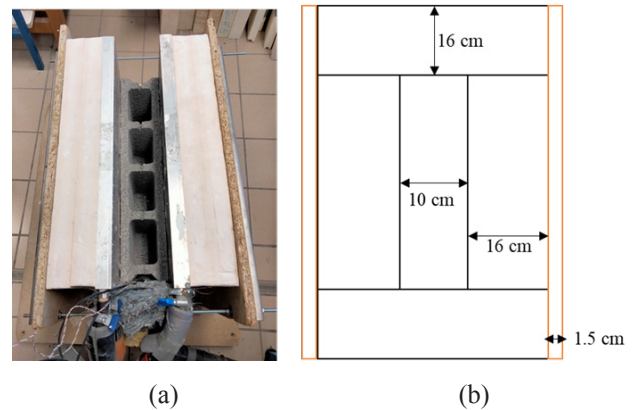


Figure 7. Photography (a) and schematic cross section (b) of the experimental setup

3.1.1 Measuring Devices

A thermocouple is a sensor that consists of measuring the temperature at a particular point, i.e. it is used to measure the temperature in the form of an electric current or an electromotive force. This measurement is based on

the Seebeck effect.

Indeed, a thermocouple is composed by two wires of different metals which are joined at the ends. Then, the latter creates a junction so that the temperature is measured. There are different types of thermocouples, each corresponding to a different temperature range and a different accuracy.

In our experiment we used T-type thermocouples (Copper-Constantan), in order to measure the temperature in the cavities and on both sides of the block. This thermocouple is suitable for a temperature range between $-250\text{ }^{\circ}\text{C}$ and $400\text{ }^{\circ}\text{C}$. It can be used at a low temperature, such as in cryogenic applications.

The block is placed vertically between two aluminum plates, such that each plate is connected to a thermostat bath. Each bath is set at a different temperature; the first is at $10\text{ }^{\circ}\text{C}$ and the other one varies between $10\text{ }^{\circ}\text{C}$ and $50\text{ }^{\circ}\text{C}$. Then, 16 T-type thermocouples were placed in the cavities of the block using small wooden rods and on the faces of the cavities. Finally, these thermocouples are connected to an acquisition center to determine the temperature variation inside the cavities.

3.1.2 Distribution of the Sensors

16 T-type thermocouples were placed; 5 thermocouples (12, 13, 14, 15 and 16) are placed at 9 cm at the end of the block such that 3 of them are placed in the cavities (13, 14 and 15). In addition, 6 thermocouples are placed at 19 cm and 28 cm respectively from the extremity of the block (1, 2, 3, 4, 5 and 6). Finally, 5 sensors are placed at 38 cm from the extremity of the block; such that 7 and 11 are placed on the faces of the block respectively and 8, 9 and 10 are placed in the cavities. All sensors are placed at a height of 9 cm from the vertical section of the block, as in (Figure 8).

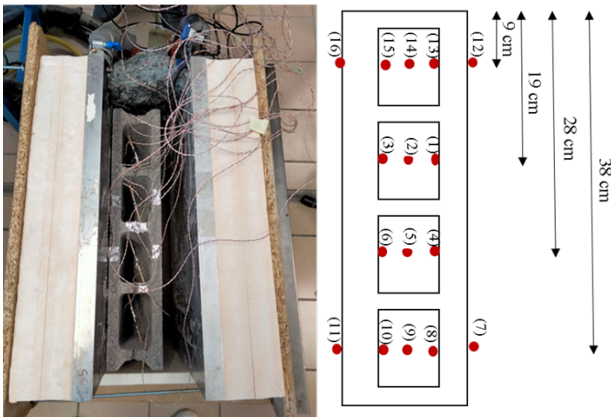


Figure 8. Distribution of thermocouples across the hollow block

3.2 Imposed Boundary Conditions

Temperature boundary conditions (Dirichlet conditions θ_1 and θ_2) were applied on the two faces of the block through heat exchange plates connected to thermostatic baths. While θ_1 remains constant approximately at $20\text{ }^{\circ}\text{C}$, θ_2 varies in a steep temperature profile between $20\text{ }^{\circ}\text{C}$ and $50\text{ }^{\circ}\text{C}$ over a period of 5 days. Moreover, the comparison between the experimental and numerical results was given a particular attention.

3.3 Numerical Model

Numerical simulations were carried out using COMSOL® version 5.6 software. In this 3D study, a structured mesh was considered using transient heat transfer.

Other the understand of the heat transfers by convection and thermal radiation that are taken into account in our numerical model on this type of concrete block that contains four rectangular cavities, the difficulty and interest of our study is the air flow inside the cavities, considering the natural convection as a laminar flow. Therefore, two physical parameters have been considered in our model; “Laminar Flow” and “Heat Transfer in Fluids”. The continuity, Navier-Stokes and energy equations have been used in our model.

The 3D block model is the same as the experimentally tested block; it is composed of a row of four rectangular cavities of $9.5 \times 19 \times 6\text{ cm}^3$. The external dimensions of the block are $49 \times 19 \times 10\text{ cm}^3$ (Figure 9).

The size, dimensions and boundary conditions of the block in the numerical analysis are identical to the experimental in transient regime. An initial condition of $\theta_0 = 20\text{ }^{\circ}\text{C}$ and a time step of 1 min were considered. The sensors are placed in the numerical model are the same as the ones placed in the experimental analysis with the aim of comparing the results of these two analyses.

The heat transfer simulation in hollow blocks is based on the thermal properties of the concrete mixture presented in Table 1. A coupled CFD-thermal analysis was adopted in order to account the three key heat transfer mechanisms of the (i.e., conduction, convection, and radiation).

The conduction occurs in the solid concrete mixture of the hollow block, while convection and radiation occur inside the block cavities. The air circulation inside the cavity (Figure 9a), promoting the natural convection, was considered as a laminar flow. It is coupled with the radiation model using the discrete ordinates method (DO) and the simulation was performed using the implicit solver of COMSOL Multiphysics®. The air density was assumed to be dependent on pressure and temperature varying according to the ideal gas relation [22-24].

The equivalent thermal properties of the solid part of the block; $\lambda=1.6W/m.K$ and $C_p=1392.82 J/Kg.K$ have been taken into account in our numerical models (Figure 9b).

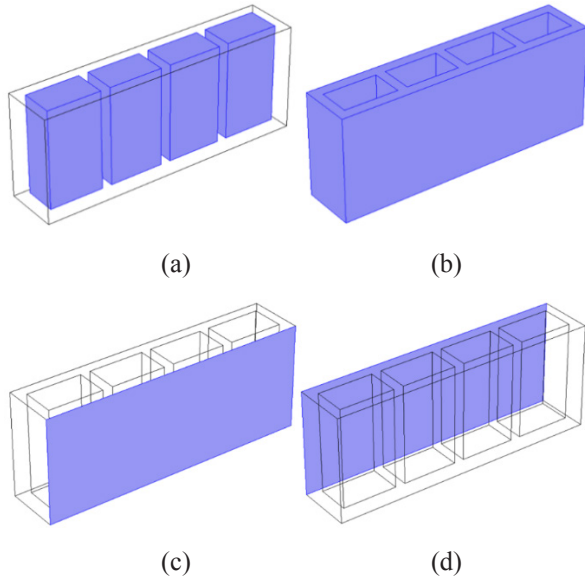


Figure 9. Materials constituting the block air (a) concrete (b) and boundary conditions θ_1 (c) et θ_2 (d)

The boundary conditions that we have considered are the boundary conditions of those of the experimental part; θ_1 and θ_2 (Figure 9c and Figure 9d).

In order to compare the experimental measurements of temperature and heat flux in the hollow block with the numerical 3D simulations, the numerical model sensors were placed at the same coordinates as those of the experimental setup. Figure 10 shows the location of sensors S2, S4, and S11 as example.

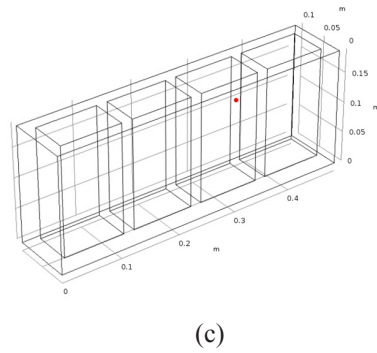
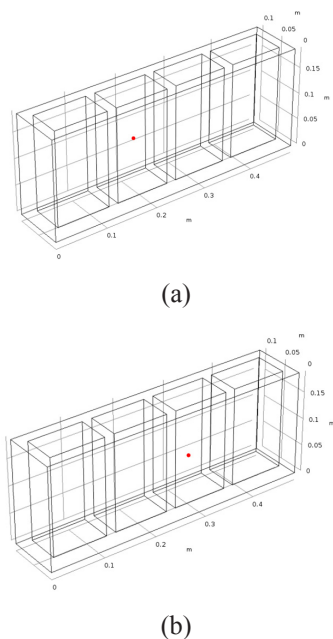


Figure 10. Sensor coordinates S2 (a) S4 (b) S11 (c)

3.4 Comparison between the Numerical and Experimental Results

The main objective of comparing numerical and experimental results is providing a solid understanding of the heat flux in hollow blocks in dynamic conditions at the boundaries of the hollow block as well as at its mesostructured (inside the cavities).

Figure 11 and Figure 12 show the evolution of temperature at the left and right boundaries of the block. The numerical results and the experimental measurements present a very good agreement. The results also show that the temperature is relatively uniform at the block edges since the difference between θ_2 , S11, and S16 does not exceed 2 degrees. This slight difference is due to the edge effects; indeed, the small size of the studied sample prevents the variation of the heat flux to be perfectly unidirectional. The same differences are observed between sensors θ_1 , S7, and S12.

The temperature on the left side increases and presents a step form due to the increase in the heat exchanging plates reference temperature (step profile 20 °C-30 °C-40 °C-50 °C); the temperature on the right side is slightly affected since it shows a little increase while the heat exchanging plate at that side is maintained at 20 °C.

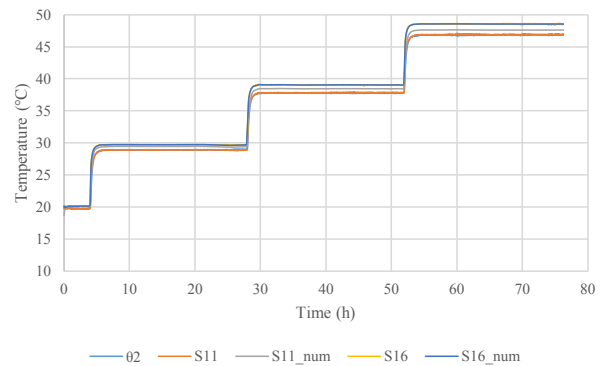


Figure 11. Comparison between numerical and experimental temperatures of sensors 11 and 16 at the left boundary of the block

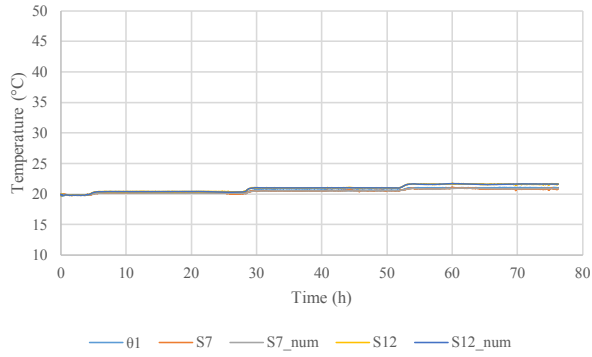


Figure 12. Comparison between numerical and experimental temperatures of sensors 7 and 12 at the right boundary of the block

The temperature measurements inside the cavities are shown in Figure 13, Figure 14, and Figure 15. The edge effects are more pronounced at the internal edges of the cavities (left and right side) and almost absent in the middle of the cavities.

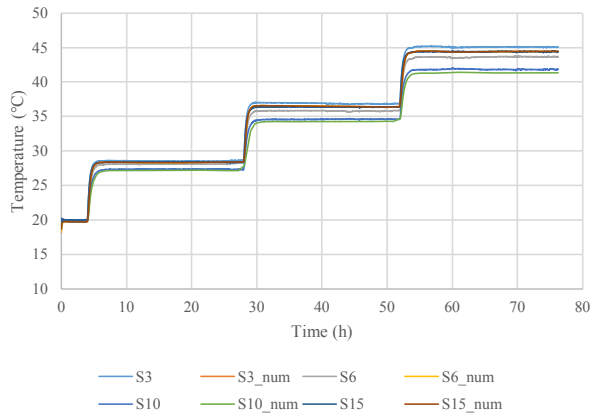


Figure 13. Comparison between numerical and experimental temperatures of sensors 3, 6, 10 and 15 at the left internal edge of the cavities

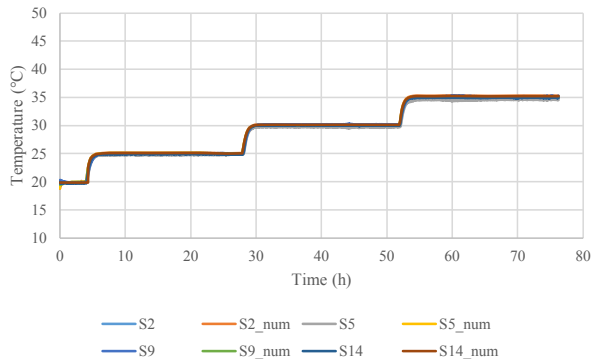


Figure 14. Comparison between numerical and experimental temperatures of sensors 2, 5, 9 and 14 at the middle of the block cavities

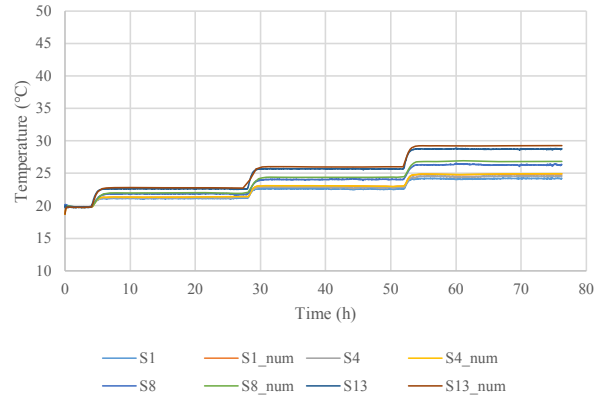


Figure 15. Comparison between numerical and experimental temperatures of sensors 1, 4, 8 and 13 at the right internal edge of the cavities

The heat flux measurements on the two interfaces of the block/heat exchanging plates were compared to numerical simulations (Figure 15). The results of the heat flux evolution are very comparable for the two sides of the hollow block. While the heat flux from the hot side peaks for each change in the temperature range and then decreases until reaching a new constant range, the heat flux from the cold side (20 °C) increases in a smoother way until reaching the new steady state value for each increase of the temperature range from the hot side. Furthermore, the computation of the numerical and experimental thermal resistances obtained from the numerical and experimental results respectively and reported in Table 2 show a great adequacy with a relative difference less than 4% for the three measurement ranges. The thermal resistance decreases with the increase of the temperature difference between the two boundaries of the hollow block from 0.148 m².K/W to 0.135 m².K/W in the numerically simulated block and from 0.142 m².K/W to 0.131 m².K/W for the experimental measurements. These results are also in compliance with the previous similar studies performed on similar hollow block with two rows of elliptical cavities [22] where the thermal resistance of a 10 cm × 20 cm × 40 cm hollow block was found equal to 0.151 m².K/W and in compliance with French thermal regulations RT 2012 [25] stating that the thermal resistance of a 10 cm × 20 cm × 50 cm hollow block with one row of squared hollows shall be taken equal to 0.12 m².K/W.

The conclusions drawn from the experimental and numerical comparisons are as follows:

A good match between numerical and experimental results can be confirmed which consolidates the numerical model allowing further investigations of heat transfer in hollow blocks having different shapes and different concrete mixtures.

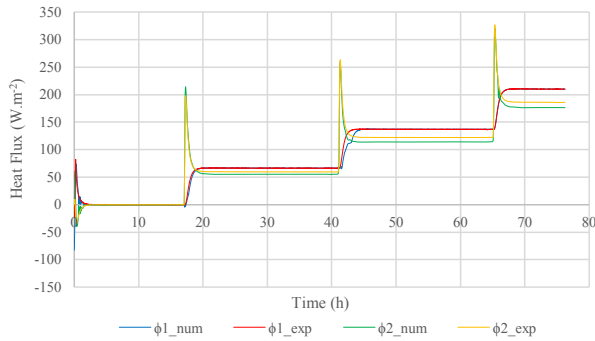


Figure 15. Comparison between numerical and experimental heat fluxes at 13 at the external faces of the hollow block

Table 2. Thermal properties of the tested materials

Temperature (°C)	20-30 °C	20-40 °C	20-50 °C
$R_{\text{experimental}}$ (m ² .K/W)	0.142	0.135	0.131
$R_{\text{numerical}}$ (m ² .K/W)	0.148	0.140	0.135
Relative deviation	4%	4%	2%

The temperature gradient inside the block decreases progressively from the side where the step temperature θ_2 is applied to the side where a constant temperature θ_1 is imposed.

The heat flux on the two boundaries of the tested hollow block was also measured and simulated showing comparable results.

Edge effects are observed at the boundaries of the block and at the internal edges of the cavities and are almost absent in the middle of the cavities. These effects can be reduced by working on a wall scale (masonry walls).

The thermal resistance of the block was always investigated for different temperature ranges and using both experimental measurements and numerical simulations showing a very high adequacy between the numerical and experimental values.

4. Conclusions

This work provides an in-depth understanding of heat transfer in hollow concrete blocks by investigating the local temperature distribution and heat flux through an experimented hollow block with rectangular cavities using the fluxmetric method under controlled conditions in a well-insulated experimental box.

The thermal properties of the hollow block and the solid matrix were first determined using a standard thermal characterization setup. Two tests were made; in the 1st test the two fluxmeters were placed in the middle of the tested block facing the bulkheads on both sides, whereas in the 2nd test, the two flux meters were placed facing the

centers of the cavities on both sides.

In the second section of the paper, a detailed thermal analysis of the hollow block was performed by imposing a constant temperature condition on one side of the block, the other side being imposed to a step temperature profile which varying between 20 °C and 50 °C. The hollow block that was placed vertically between the heat exchanging plates and sixteen thermocouples and two fluxmeters were distributed inside and at the boundaries of the block to record the temperature and heat flux evolution.

A numerical study was also performed to support and validate the measurements; a 3D model of the block was produced and numerical sensors were placed in the same locations as the experimental configuration.

After validating the heat transfer experimental and numerical models, the scope of the upcoming work will be to improve the thermal performance of the block by modifying the concrete mixture composition, or by modifying the block internal geometry, or by filling the block cavities by insulation materials.

Conflict of Interest

There is no conflict of interest.

References

- [1] Energie, changement climatique et bâtiment en Méditerranée : étude nationale Liban - Plan-bleu : Environnement et développement en Méditerranée. <https://planbleu.org/publications/energie-changement-climatique-et-batiment-en-mediterranee-etude-nationale-liban/>
- [2] del Coz Díaz, J.J., García Nieto, P.J., Domínguez Hernández, J., et al., 2010. A FEM comparative analysis of the thermal efficiency among floors made up of clay, concrete and lightweight concrete hollow blocks. *Applied Thermal Engineering*. 30(17), 2822-2826. DOI: <https://doi.org/10.1016/j.applthermaleng.2010.07.024>
- [3] Ribeiro, R.S., Sousa, R.P.D., Amarilla, R.S.D., et al., 2021. Sound insulation of a hollow concrete blocks wall made with construction and demolition waste and wood-based panels as linings. *Building Acoustics*. 28(4), 423-442. DOI: <https://doi.org/10.1177/1351010X21993640>
- [4] Fringuellino, M., Smith, R.S., 1999. Sound Transmission through Hollow Brick Walls. *Building Acoustics*. 6(3), 211-224. DOI: <https://doi.org/10.1260/1351010991501419>
- [5] Yang, W., Mai, G., Yang, R., 2004. Study of sound

- insulation properties of concrete hollow brick wall. <https://www.semanticscholar.org/paper/STUDY-OF-SOUND-INSULATION-PROPERTIES-OF-CONCRETE-Yang-Mai/a428e48490ca7694b5b-31c75058fd50bcea6a5aa>.
- [6] Fraile-Garcia, E., Ferreiro-Cabello, J., Defez, B., et al., 2016. Acoustic Behavior of Hollow Blocks and Bricks Made of Concrete Doped with Waste-Tire Rubber. *Materials (Basel)*. 9(12), 962. DOI: <https://doi.org/10.3390/ma9120962>
- [7] del Coz Díaz, J.J., García Nieto, P.J., Domínguez Hernández, J., et al., 2009. Thermal design optimization of lightweight concrete blocks for internal one-way spanning slabs floors by FEM. *Energy and Buildings*. 41(12), 1276-1287. DOI: <https://doi.org/10.1016/j.enbuild.2009.08.005>
- [8] Antar, M.A., Baig, H., 2009. Conjugate conduction-natural convection heat transfer in a hollow building block. *Applied Thermal Engineering*. 29(17), 3716-3720. DOI: <https://doi.org/10.1016/j.applthermaleng.2009.04.033>
- [9] Urban, B., Engelmann, P., Kossecka, E., et al., 2011. Arranging Insulation for Better Thermal Resistance in Concrete and Masonry Wall Systems. 3, 8.
- [10] Mahmoud, M., Ben-Nakhi, A., Ben-Nakhi, A., et al., 2012. Conjugate conduction convection and radiation heat transfer through hollow autoclaved aerated concrete blocks. *Journal of Building Performance Simulation*. 5(4), 248-262. DOI: <https://doi.org/10.1080/19401493.2011.565886>
- [11] Manz, H., 2003. Numerical simulation of heat transfer by natural convection in cavities of facade elements. *Energy and Buildings*. 35(3), 305-311. DOI: [https://doi.org/10.1016/S0378-7788\(02\)00088-9](https://doi.org/10.1016/S0378-7788(02)00088-9)
- [12] Fogiatto, M.A., Santos, G.H., Mendes, N., 2016. Thermal transmittance evaluation of concrete hollow blocks. Undefined. [online]. Available on: <https://www.semanticscholar.org/paper/Thermal-transmittance-evaluation-of-concrete-hollow-Fogiatto-Santos/f59a619a72d9a1b0640e6e75189c434fd33be95d>
- [13] Zhang, Y., Wang, Q., 2017. Influence of Hollow Block's Structural Configuration on the Thermal Characteristics of Hollow Block Wall. *Procedia Engineering*. 205, 2341-2348. DOI: <https://doi.org/10.1016/j.proeng.2017.10.306>
- [14] Al-Tamimi, A.S., Baghabra Al-Amoudi, O.S., Al-Osta, M.A., et al., 2020. Effect of insulation materials and cavity layout on heat transfer of concrete masonry hollow blocks. *Construction and Building Materials*. 254, 119300. DOI: <https://doi.org/10.1016/j.conbuildmat.2020.119300>
- [15] Al-Tamimi, M., Al-Osta, O., Al-Amoudi, R., et al., 2017. Effect of Geometry of Holes on Heat Transfer of Concrete Masonry Bricks Using Numerical Analysis. *Arabian Journal for Science & Engineering*. 42. DOI: <https://doi.org/10.1007/s13369-017-2482-6>
- [16] Xamán, J., Cisneros-Carreño, J., Hernández-Pérez, I., et al., 2017. Thermal performance of a hollow block with/without insulating and reflective materials for roofing in Mexico. *Applied Thermal Engineering*. 123, 243-255. DOI: <https://doi.org/10.1016/j.applthermaleng.2017.04.163>
- [17] Chihab, Y., Essaleh, L., Bouferra, R., et al., 2021. Numerical study for energy performance optimization of hollow concrete blocks for roofing in a hot climate of Morocco. *Energy Conversion and Management*. 12, 100113. DOI: <https://doi.org/10.1016/j.ecmx.2021.100113>
- [18] del Coz Díaz, J.J., García Nieto, P.J., Álvarez Rabanal, F.P., et al., 2011. Design and shape optimization of a new type of hollow concrete masonry block using the finite element method. *Engineering Structures*. 33(1), 1-9. DOI: <https://doi.org/10.1016/j.engstruct.2010.09.012>
- [19] Hu, W., Xia, Y., Li, F., et al., 2021. Effect of the filling position and filling rate of the insulation material on the insulation performance of the hollow block. *Case Studies in Thermal Engineering*. 26, 101023. DOI: <https://doi.org/10.1016/j.csite.2021.101023>
- [20] Wu, J., Bai, G., Zhao, H., et al., September 2015. Mechanical and thermal tests of an innovative environment-friendly hollow block as self-insulation wall materials. *Construction and Building Materials*. 93, 342-349. DOI: <https://doi.org/10.1016/j.conbuildmat.2015.06.003>
- [21] National standards and national normative documents, July 2001. Thermal performance of building materials and products - Determination of thermal resistance by means of guarded hot plate and heat flow meter methods - Dry and moist products of medium and low thermal resistance.
- [22] Sassine, E., Cherif, Y., Dgheim, J., et al., 2020. Experimental and Numerical Thermal Assessment of Lebanese Traditional Hollow Blocks. *International Journal of Thermophysics*. 41(4), 47. DOI: <https://doi.org/10.1007/s10765-020-02626-7>
- [23] Sassine, E., Cherif, Y., Dgheim, J., et al., 2020. Experimental and Numerical Thermal Assessment of

- EPS Concrete Hollow Blocks in Lebanon. *Journal of Materials in Civil Engineering*. 32(8), 05020007.
DOI: [https://doi.org/10.1061/\(ASCE\)MT.1943-5533.0003335](https://doi.org/10.1061/(ASCE)MT.1943-5533.0003335)
- [24] Sassine, E., Cherif, Y., Dgheim, J., et al., 2020. Investigation of the mechanical and thermal performances of concrete hollow blocks. *SN Applied Sciences*. 2(12), 2006.
DOI: <https://doi.org/10.1007/s42452-020-03881-x>
- [25] RÉGLEMENTATION THERMIQUE, 2012. RÈGLES Th-U, FASCICULE 4: PAROIS OPAQUES, CSTB.